arXiv:nucl-th/0307044v1 10 Jul 2003

Non-locality and Medium Effects in the Exclusive Photoproduction of η Mesons on Nuclei*

M. Hedayati-Poor[a,c], S. Bayegan[b] and H.S. Sherif[a]

(a)Department of Physics, University of Alberta

Edmonton, Alberta, Canada T6G 2J1

(b)Department of Physics, University of Tehran, Iran

(c)Department of Physics, University of Arak, Iran

(February 8, 2008)

Abstract

A relativistic model for the quasifree exclusive photoproduction of η mesons on nuclei is extended to include both non-local and medium effects. The reaction is assumed to proceed via the dominant contribution of the $S_{11}(1535)$ resonance. The complicated integrals resulting from the non-locality are simplified using a modified version of a method given by Cooper and Maxwell. The non-locality effects are found to affect the magnitude of the cross section. Some possibilities reflecting the effects of the medium on the propagation and properties of the intermediate S_{11} resonance are studied. The effects of allowing the S_{11} to interact with the medium via mean field scalar and vector potentials are considered. Both broadening of width and reduction in mass of the resonance lead to a suppression of the calculated cross sections.

PACS number(s) 25.20.Lj, 24.10.Jv, 14.20.Gk, 13.60.Le

*Work supported in part by the Natural Sciences and Engineering Research Council of Canada

I. INTRODUCTION

The photoproduction of the eta mesons on nucleons and nuclei is a subject of current interest. The production on nucleons provides an opportunity to study nucleon resonances in the second resonance region. In the past decade there have been a large number of studies, both theoretical and experimental, on the reaction on nucleons and deuterons and much has been learned [1–4].

Photoproduction on nuclei can be valuable in learning about the changes in hadron properties in the nuclear medium. Inclusive photoproduction cross sections for a number of nuclei have been measured at MAMI by Roebig-Landau *et al.* [5] and recently at INS by Yorita *et al.* [6]; data on coherent reactions are confined to the lightest nuclei. No data have been reported however on quasifree or incoherent photoproduction. Part of the reason for this is the smallness of the cross sections for these processes [7,8]. It is therefore imperative that efforts should continue in the direction of improving the theoretical calculation, both for their own sake and also for better guidance to experiments.

In an earlier study we presented a relativistic model for exclusive and inclusive photoproduction of eta mesons on nuclei [9,10]. This study was extended to incoherent photoproduction in ref. [11]. The model is based on an effective Lagrangian to describe the production mechanism [1]. It includes contributions from nucleon resonances in the second resonance region, from nucleon pole diagrams and from vector meson diagrams. This approach has proved successful in describing the experimental data for the elementary reaction. The other key ingredients of the study on nuclei are the use of relativistic mean field dynamics to treat the nucleon motion and to allow for final state interactions of the outgoing particles with the residual nucleus.

In the earlier studies, two key approximations were applied to simplify the calculation of the reaction amplitudes. The first of these was a local approximation for the propagators. The other approximation was to use a free (undressed) form for the propagators, in which the interactions of the propagating particles with the nuclear medium were ignored.

Non-locality effects in coherent photoproduction of pions and eta mesons on nuclei have been studied, in a relativistic model, by Peters *et al.* [8,12]. For the pion production case these authors also investigated the medium modifications of the nucleon and delta propagators. For the coherent photoproduction of eta mesons it was established that non-local effects can lead to enhancement of the contribution of the S_{11} resonance which appeared to be strongly suppressed in earlier local calculations [7,13].

The present study is concerned with the investigation of non-local and medium effects in the quasifree photoproduction of eta mesons on nuclei, i.e. reactions of the type $A(\gamma, \eta p)B$. In this sense it complements the work of Peters *et al.*, on coherent photoproduction. Even though the cross section for the quasifree photoproduction reaction is rather small, it serves as a proto-type for studying these effects. Moreover its amplitude is the main building block, in at least some models [10,14], for calculating inclusive cross sections.

Earlier relativistic and non-relativistic studies of the quasifree photoproduction [9,14] show clearly that the reaction is strongly dominated, at the energies not too far from threshold, by the S_{11} resonance. We therefore restrict the present study to the dominant S_{11} contributions.

In the next section we discuss the formalism for improving our previous model [9] (henceforth referred to as I), to include both non-locality and possible medium effects on the resonance. The results and discussions are given in section III and the conclusion in section IV.

II. FORMALISM

In I, starting from a relativistic interaction Lagrangian for a system of photons, nucleons and mesons, we obtained a transition amplitude for the A(γ, ηp)A-1 reaction. To simplify the calculations a local approximation was adopted and free propagators were used for the intermediate resonances (see I for details). In the present treatment both approximations will be dropped. It is assumed here that the production of eta meson takes place through

formation and subsequent decay of the $S_{11}(1535)$ resonance.

A. The Non-local Reaction Amplitude

At the tree-level the S-matrix for the A($\gamma,\ \eta p$)A-1 reaction, through the S_{11} resonance, can be cast in the following from [9],

$$
\begin{aligned}
S_{fi} = & \frac{e}{(2\pi)^{17/2}} \frac{\kappa_R^p g_{\eta NR}}{M+M_R} \left(\frac{M}{E_p} \frac{1}{2\omega_\eta} \frac{1}{2\omega_\gamma} \right)^{1/2} \sum_{J_B M_B} (J_f, J_B; M_f, M_B | J_i, M_i) \left[S_{J_i J_f}(J_B) \right]^{\frac{1}{2}} \\
& \times \{ \int d^4x d^4y d^4p \ \bar{\psi}_{sf}(y) \phi_\eta(y) \frac{e^{-ip(y-x)}}{\not{p} - M_R + i\frac{\Gamma}{2}} \gamma_5 \not{k}_\gamma \not{\epsilon} \ e^{ik_\gamma x} \psi_B(x) \\
& + \int d^4x d^4y d^4p \ \bar{\psi}_{sf}(y) \gamma_5 \not{k}_\gamma \not{\epsilon} \ e^{ik_\gamma y} \frac{e^{-ip(y-x)}}{\not{p} - M_R + i\frac{\Gamma}{2}} \phi_\eta(x) \psi_B(x) \ \}, \qquad (2.1)
\end{aligned}
$$

where $S_{J_i J_f}(J_B)$ and $(J_f, J_B; M_f, M_B | J_i, M_i)$ are spectroscopic and Clebsh-Gordon coefficients, respectively. M, M_R and Γ are the nucleon mass, resonance mass and width, respectively. E_P, ω_η and ω_γ are the energies of the outgoing proton, eta meson and incident photon, respectively. κ_R^p and $g_{\eta NR}$ are the anomalous magnetic moment of the resonance and the coupling constant of the eta-nucleon-resonance vertex. $\psi_{sf}(y)$, $\psi_B(y)$ and $\phi_\eta(y)$ are wave functions of the outgoing proton, the bound (initial state) proton and the eta meson, respectively. The ψ's are solutions of Dirac equations with appropriate mean field potentials and ϕ is a solution of the Klein - Gordon equation. Instead of the local approximation used in I (this approximation is exact in the limit where both ψ_{sf} and ϕ_η are plane waves), we perform a complete non-local calculation.

The integrals in (2.1) can be computed as they stand, but it is possible to follow a somewhat simpler approach [15]. We rewrite the two integrals in (2.1) as,

$$
\mathcal{I} = (2\pi)^4 \int d^4y \ \bar{\psi}_{sf}(y) \phi_\eta(y) W^s(y) + (2\pi)^4 \int d^4y \ \bar{\psi}_{sf}(y) \gamma_5 \not{k}_\gamma \not{\epsilon} \ e^{ik_\gamma y} W^u(y), \qquad (2.2)
$$

where

$$
\begin{aligned}
(2\pi)^4 W^s(y) &= \int d^4x d^4p \frac{e^{-ip(y-x)}}{\not{p} - M_R + i\frac{\Gamma}{2}} \gamma_5 \not{k}_\gamma \not{\epsilon} \ e^{ik_\gamma x} \psi_B(x) \\
(2\pi)^4 W^u(y) &= \int d^4x d^4p \frac{e^{-ip(y-x)}}{\not{p} - M_R + i\frac{\Gamma}{2}} \phi_\eta(x) \psi_B(x), \qquad (2.3)
\end{aligned}
$$

where the superindices refer to s- and u-channel diagrams. If we act from the left with the operator $\not{p} - M_R + i\frac{\Gamma}{2}$ and then carry the integration over momentum, we obtain the following Dirac-type linear differential equation,

$$(\not{p} - M_R + i\frac{\Gamma}{2})W^i(y) = V^i(y), \tag{2.4}$$

where the source terms for s- and u-channels are, respectively,

$$\begin{aligned} V^s(y) &= \gamma_5 \not{k}_\gamma \not{\epsilon} \, e^{ik_\gamma y}\psi_B(y) \\ V^u(y) &= \phi_\eta(y)\psi_B(y). \end{aligned} \tag{2.5}$$

After taking care of the time dependence, equation (2.4) leads to the following second order differential equation for the space part of the upper component of W^i (which we denote $W^i_{up}(\mathbf{r})$; note it continues to be spin dependent and similarly for $V^i(\mathbf{r})$). The lower component of $W^i(\mathbf{r})$ can be obtained from its upper component (see below).

$$-\mathbf{p}^2 W^i_{up}(\mathbf{r}) + \alpha\beta W^i_{up}(\mathbf{r}) = \beta V^i_{up}(\mathbf{r}) - \sigma\cdot\mathbf{p} V^i_d(\mathbf{r}), \tag{2.6}$$

where the indices up and d indicate the upper and lower components of the functions W^i and V^i. The α's and β's are given by,

$$\begin{aligned} \alpha^s &= E_b + w_\gamma - M_R + i\frac{\Gamma}{2} \\ \beta^s &= E_b + w_\gamma + M_R - i\frac{\Gamma}{2} \\ \alpha^u &= E_b - w_\eta - M_R + i\frac{\Gamma}{2} \\ \beta^u &= E_b - w_\eta + M_R - i\frac{\Gamma}{2}, \end{aligned} \tag{2.7}$$

where E_b is the energy of the bound nucleon. The following expansions are used for $W^i_{up}(\mathbf{r})$ and the source part of equation (2.6) (we drop the index i for now),

$$\begin{aligned} W_{up}(\mathbf{r}) &= \sum_{L,M,J} \frac{w^M_{LJ}(r)}{r}\mathcal{Y}^M_{L\frac{1}{2}J}(\Omega) \\ V_{up}(\mathbf{r}) - \beta\sigma\cdot\mathbf{p}V_d(\mathbf{r}) &= \sum_{L,M,J} \frac{\xi^M_{LJ}(r)}{r}\mathcal{Y}^M_{L\frac{1}{2}J}(\Omega). \end{aligned} \tag{2.8}$$

Substituting the above expansions into (2.6) leads to the following second order radial differential equation,

$$\left[\frac{d^2}{dr^2} - \frac{L(L+1)}{r^2} + \alpha\beta\right] w^M_{LJ}(r) = \xi^M_{LJ}(r). \tag{2.9}$$

The presence of the resonance's width in equation (2.4) makes both α and β complex. The equation above, in the limit of no source, is similar to the Bessel equation with a complex variable. The complexity of the argument requires care in the choice of boundary conditions to insure proper asymptotic behavior. In the presence of sources the solutions must be matched to combinations of Bessel and Neumann type functions, which vanish at large distances. The above equation can be solved by a number of different methods. The method which we adopt here is the Gauss elimination matrix [15]. This method is suitable for solving the differential equation (2.9) with the boundary condition mentioned above.

Substituting eq.(2.3) into eq.(2.1) and using partial wave expansions of all wave functions [16], the S-matrix in the distorted wave approximation (DWA) can be written as,

$$\begin{aligned}
S_{fi} = & \frac{e}{\pi}\frac{1}{(4\pi)^{\frac{1}{2}}}\left(\frac{E_p+M}{E_p\omega_\eta\omega_\gamma}\right)^{1/2}\frac{\kappa^p_R g_{\eta NR}}{M+M_R}\delta(E_B+\omega_\gamma-E_p-\omega_\eta) \\
& \times \sum_{J_B M_B}(J_f,J_B;M_f,M_B|J_i,M_i)\left[\mathcal{S}_{J_iJ_f}(J_B)\right]^{1/2} \\
& \times \sum_{LJM} i^{-L}Y_L^{M-s_f}(\hat{k}_f)\,(L,1/2;M-s_f,s_f|J,M) \\
& \times \Bigg\{ \sum_{L_\eta,M_\eta} i^{-L_\eta}\left[Y^{M_\eta}_{L_\eta}(\hat{k}_\eta)\right]^* \\
& \times \int d^3y \left[\mathcal{Y}^M_{L,1/2,J}(\Omega)\right]^* \left[f_{LJ}(r) \quad i\sigma\cdot\hat{\mathbf{r}}\,g_{LJ}(r)\right] v_{L_\eta}(r) Y^{M_\eta}_{L_\eta}(\Omega) \begin{bmatrix} W^s_{up} \\ W^s_d \end{bmatrix} \\
& + \sum_{L_\gamma}\left[\frac{2L_\gamma+1}{4\pi}\right]^{\frac{1}{2}} i^{L_\gamma} \\
& \times \int d^3r \left[\mathcal{Y}^M_{L,1/2,J}(\Omega)\right]^* \left[f_{LJ}(r) \quad i\sigma\cdot\hat{\mathbf{r}}\,g_{LJ}(r)\right] j_{L\gamma}(k_\gamma r) Y^0_{L_\gamma}(\Omega)\gamma_0\gamma_5 \not{\epsilon}_\gamma \begin{bmatrix} W^u_{up} \\ W^u_d \end{bmatrix} \Bigg\},
\end{aligned} \tag{2.10}$$

where $f_{LJ}(r)$, $g_{LJ}(r)$ are the upper and lower component radial wave functions of the outgoing nucleon, respectively. $v_{l_\eta}(r)$ describes the radial wave function of the eta meson. The

expansions of the upper components of W^i are given in equation (2.8). The lower components W^i_d are related to the upper components by,

$$W^i_d(\mathbf{r}) = \frac{\sigma \cdot \mathbf{p} W^i_{up}(\mathbf{r}) - V^i_d(\mathbf{r})}{\beta_i}. \tag{2.11}$$

B. Inclusion of Medium Effects

The properties of the resonances are expected to change in the nuclear medium. The two properties of interest are mass and width. It is often argued that the mass of the nucleon is changed in the medium, and in the spirit of the Walecka model [17], this could be effected by the scalar field. Thus our first attempt is to let the S_{11} resonance interact with the nuclear medium through the nuclear scalar and vector potentials. The formalism discussed in the previous subsection can be modified to include these nuclear mean fields in the resonance propagator. We modify equation (2.4) by subtracting the vector potentials from the zeroth component of the resonance 4-momentum and adding the scalar potentials to its mass,

$$(\not{p} - \gamma^0 U_v(y) - M_R - U_s(y) + i\frac{\Gamma}{2}) W^i(y) = V^i(y). \tag{2.12}$$

The differential equation obtained from (2.12) is somewhat different from (2.9); the parameters α and β are now functions of r. The equation has the form,

$$\Big[\frac{d^2}{dr^2} - \frac{l(l+1)}{r^2} + \alpha(r)\beta(r) + (\kappa(l)+1)\frac{\beta'(r)}{r\beta(r)} + \frac{\beta''(r)}{2\beta(r)} - \frac{3}{4}(\frac{\beta'(r)}{\beta(r)})^2\Big] y^M_{lJ}(r) = \tag{2.13}$$
$$\sqrt{\beta(r)}\tau^M_{lJ}(r) + i\frac{\beta'(r)}{\beta^{\frac{3}{2}}(r)}\zeta^M_{l'J}(r) - i\frac{1}{\beta^{\frac{1}{2}}(r)}\zeta'^M_{l'J}(r) + i\frac{\kappa(l')+1}{r\beta^{\frac{1}{2}}(r)}\zeta^M_{l'J}(r),$$

where $w^M_{lJ}(r) = \sqrt{\beta(r)} y^M_{lJ}(r)$ and the function $\kappa(l)$ is defined as

$$\begin{aligned} \kappa(l) &= l+1 \qquad \text{for} \qquad J = l + \frac{1}{2} \\ \kappa(l) &= -l-1 \qquad \text{for} \qquad J = l - \frac{1}{2}, \end{aligned} \tag{2.14}$$

and $l' = 2J - l$.

The inclusion of the interaction with the medium also necessitates that the expansion of the source functions (eq.(2.8)) be done for the upper and lower components separately,

$$V_{up}(\mathbf{r}) = \sum_{l,M,J} \frac{\tau_{lJ}^{M}(r)}{r} \mathcal{Y}_{l\frac{1}{2}J}^{M}(\Omega)$$
$$V_{d}(\mathbf{r}) = \sum_{l,M,J} \frac{\zeta_{lJ}^{M}(r)}{r} \mathcal{Y}_{l\frac{1}{2}J}^{M}(\Omega). \tag{2.15}$$

The second order radial differential equation (2.13) is again solved using the gauss elimination matrix method mentioned above. The lower components of the W^i are obtained from their upper components using equation (2.11). The rest of the calculations proceed along the same lines as the non-locality ones of subsection II A.

The influence of the medium may also be formulated in terms of changes in the resonance properties such as mass and width. These changes are likely to be density dependent. When this is the case, these changes can be accomodated in the calculation of the reaction amplitude in essentially the same manner as the above treatment of interaction potentials. The implementation of non-density-dependent changes is of course much simpler.

III. RESULTS AND DISCUSSION

In this section we investigate the impact of doing non-local calculations on the cross section for the quasifree production. We also consider a number of options that would simulate the medium effects on the propagating S_{11} resonance and asses how these affect the calculated cross sections.

In I we have investigated the kinematical conditions under which the calculated cross sections are optimal. It was concluded that a symmetric arrangement for detecting the outgoing proton and eta meson at 30^o on both sides of the incident beam led to the maximum cross section on ^{12}C at 750 MeV. We shall adopt this geometry in all the calculations presented here. In addition the coupling parameters used are the same as those of I. The bound state wave functions for the initial state bound proton are calculated using the mean field Hartree potentials of Horowitz and Serot [18]. The distorted wave functions for the

outgoing protons are calculated using golobal potentials provided by Cooper *et al.* [19] and the optical potentials for eta mesons are those of Chiang *et al.* [20] with the real part of S_{11} self energy being taken to be prportional to the nuclear density.

Figure 1 shows the calculated triple differential cross section at $E_\gamma = 750$ MeV as a function of the kinetic energy of the outgoing eta meson. As pointed out earlier, a calculation in which both the proton and the eta are taken as plane waves is by necessity a local calculation. We show this by the dotted curve. The dashed curve shows the corresponding local distorted wave (DW) calculation. Comparison between these two curves establishes, as has been learned in many earlier calculations, the strong suppression of the cross sections due to final state interactions.

The solid curve in Fig.1 shows the non-local calculations. Here we find that the non-locality effects lead to increase in the cross section, but with only a slight change in shape. The increase can be as high as 25%. Figure 2 shows a similar comparison between local (dashed curve) and non-local calculations (solid curve) for ^{40}Ca at the same incident energy. The features are essentially the same as in Fig.1. Thus the increase in the cross section due to non-locality effects appears to be independent of the target nucleus.

Some theoretical approaches to the calculation of the inclusive cross sections start from calculations of the exclusive cross sections discussed here but with the wave functions of the outgoing protons taken as plane waves. Thus in these calculations only the eta wave function is distorted due to the final state interactions. The rationale for this is given, for example in ref. [10]. In Fig.3 we show the effect of non-locality on this type of calculation. We see again that the net result is an increase in the cross section in essentially the same fashion as in the two cases discussed in Figs.1 and 2.

The increase of the cross section in non-local calculations appears to be a universal feature independent of the energy of the incident photon (in the region of the S_{11} dominance). It is also present at other angular pairs of the outgoing particles provided these remain in the forward hemisphere close to where the cross section is large. It is of interest to try to understand why the inclusion of non-locality leads to an increase in the cross sections.

This feature appears to be closely connected to the final state interactions of the outgoing particles with the residual nucleus, i.e. to the distortion effects. To see this we first note that plane wave calculations in which these effects are neglected are strictly local and as seen in Fig.1 have relatively large cross sections. Local calculations with distortion effects lead to a noticeable reduction of the cross section. But the cross section increases as the non-locality is taken into consideration.

Because the cross sections are substantial only when the pair of outgoing particles are moving in a forward direction it is possible to argue that the increase is due to a reduction in the absorption of the outgoing particles in the non-local case. In the plane wave local calculations the pair is produced at the same point where the formation of the S_{11} resonance takes place; subsequently they move freely through the nuclear medium. In local distorted wave calculations they do interact with the nucleus and suffer absorption and hence the cross section is reduced (see dashed curve in Fig.1). In non-local calculations, on the other hand, the S_{11} resonance decays generally at a point different from the point of its formation. Because the motion is largely forward the outgoing particles travel in the nuclear medium for a shorter distance and hence suffer less absorption. This leads to some increase in the cross section. We have tested this interplay between absorption effects and non-local calculations by gradually scaling the distorting potentials of either particle. We found clear confirmation of this relationship between the relative increase in the cross section and the size of the distorting potentials. Note that the reason for the increase in the present quasifree reaction is quite different from the case of coherent photoproduction where the increase in the cross section due to non-locality can be understood in terms of the interplay between the nuclear structure of the target and the spin structure of the elementary amplitude [12].

We now investigate the influence on the cross section due to the medium effects on the propagating S_{11} resonance. All the calculations reported below include non-local effects as discussed above. It is generally agreed that the medium is likely to affect both the mass and the width of the resonance. We can alternatively look at these effects in a framework where they are expressed in terms of interactions of the resonance with the surrounding

nucleons. In this respect one is inclined to think of a mean field interaction modeled along the case of nucleons. It may therefore be a good starting point to consider such a case. A rough approximation is to take the interaction to be that experienced by the bound nucleon that formed the resonance, namely the scalar and vector Dirac Hartree potentials of ref. [18]. The results are displayed in Fig.4. The solid curve (No ME) represents the case of free propagation, i.e without interactions with the medium. If we include only the scalar Hartree potential S(r) in the calculations, we are then affectively changing the mass of the resonance in radially-dependent way. The result of invoking such an effective mass is shown by the dashed curve in the Fig.4. There is a large reduction in the cross section. We should add however that the Hartree scalar potential is rather deep (about 600 MeV at the centre of the nucleus) and hence the effect may be somewhat exaggerated. The dotted curve shows the results when both the Hartree vector and scalar potentials are included. We find, in this case, a much reduced effect on the cross section; the vector and scalar potentials have opposing influences. This can be understood qualitatively in terms of the opposite signs of these potentials and the structure of the propagator. The vector potential when added to the energy term tends to offset the increased gap between the energy and mass terms resulting from the reduction in mass due to the scalar potential.

Another possible way of probing the effects of the medium on the propagating resonance is to change the width of the resonance from its free space value. The calculations discussed above have all been performed using $\Gamma = 150$ MeV. In addition to uncertainties surrounding the free width, it is likely that the width will broaden in the medium; there are for example indications of some broadening in the region of the $\triangle(1232)$ resonance [21]. To test the effect of such broadening we carry out calculations using a larger value $\Gamma = 208$ MeV. This value is obtained by Breit - Wigner fits to the data of the elementary reaction [22] and is also close to the upper limit used in the analysis of ref. [6]. We also consider the effect of collision broadening of the width following a suggestion by Lehr and Mosel [23]. These authors considered a model for the broadening of the D_{13} resonance due to collisions with nucleons, in an attempt to explain the total photoabsorption cross section on nuclei. They

suggest that, to first order in the baryon density ρ, the width may be written as

$$\Gamma(\rho) = \Gamma_{\rm free} + 50\frac{\rho}{\rho^0} \tag{3.1}$$

where $\Gamma_{\rm free} = 150$ MeV and ρ^0 is the density of infinite nuclear matter (taken to be 0.17 fm^{-3}).

The results of these calculations are shown in Fig.5. We note that increasing the width from 150 to 208 MeV results in a drastic reduction (about 50% at the peaks) of the cross section. On the other hand the density dependent broadening has only a small effect (around 10%). The weakening of broadening in the surface region in this case appears to be responsible for the much reduced effect on the cross section.

The next step in looking at medium effects is to reconsider the changes in the mass of the resonance in the medium together with the change in width. Figure 6 shows comparisons involving the use of an expression for the mass borrowed from the work of Saito and Thomas [24] on the medium effects on baryon masses. One of the relations used by these authors for the change in the nucleon mass within the medium is of the form

$$M(\rho) = M_{\rm free} - 0.14\frac{\rho}{\rho^0}M_{\rm free} \tag{3.2}$$

We adopt this same expression for the mass of the S_{11}. This provides a somewhat different form for the change in mass from that used in the calculations of Fig.4 (due the scalar part of the Hartree potential). The cross section calculated with the form (3.2) for the mass is shown by the dashed curve in Fig.6. The solid curve is the result of calculations that include the above mass change as well as a change in width according to the form given in eq.(3.1). The mass dependence on the density reduces the cross section by an amount which, though substantial, is much less than what was obtained using the deep Hartree potential (Fig.4). The addition of density-dependent width broadening reduces the cross section further, similar to what was noted in Fig.5.

Finally we discuss the medium effects for the calculations shown in Fig.3, where only the final state interactions of the eta are taken into account. The comparisons shown in Fig.7

are for the density dependent mass and width changes discussed above. We see that the mass effect is larger than the width effect and that the two together lead to the smallest cross section. It is therefore likely that the net effect of the medium on inclusive reaction will be to reduce the cross sections. Detailed calculations of this are underway.

We have carried out similar calculations at $E_\gamma = 900$ MeV. The general features observed in the above figures are found to hold at this higher enery.

IV. CONCLUSION

Our earlier work on the exclusive quasifree photoproduction of eta mesons on nuclei involved two approximations in the calculations of the production amplitude. The first was a local approximation in which the absorption of the photon and the production of the eta were assumed to occur at the same point. The second approximation was to assume free propagation of the intermediate resonances; no interaction or change of properties took place in the medium. In this paper, adopting an S_{11} resonance model, we have carried out non-local calculations in order to correct for the first approximation. We have also investigated the role of medium interactions or alternatively changes in mass and width of the resonance on the calculated cross sections.

We find that the non-local effects are important for the cross section calculations. Typically these effects lead to a moderate increase in the cross sections. This feature appears to apply regardless of the target nucleus or whether the final state interactions of the proton are taken into account.

In our investigation of the influence of possible medium effects on the propagation of the S_{11} resonance we considered various possibilities. If one assumes that the resonance experiences a mean field similar to that of the nucleon then the scalar part of the mean field would act as a de-facto reduction in the mass of the resonances. We find that this term alone would lead to large suppression in the cross section if its strength is maintained at that used for nucleon binding in a Dirac - Hartree model. This suppression is found to moderate if

the vector component of the interaction is added. Note however that the Hartree potentials are known to be rather deep.

The cross sections are no doubt sensitive to the mass of the resonance. In fact we found that if the mass of the resonance is reduced by 30%, the cross section is drastically reduced. A more realistic change in the mass is that of ref. [24], based on the quark meson coupling model. In this instance also the mass is dependent on the nuclear density but in a much weaker fashion compared to that affected by the Hartree scalar potential. The cross section is reduced due to the reduction in mass; the moderate density dependence leads to a moderation in the suppression of the cross section. Increasing the width of the resonance also leads to a reduction in the cross section. If the width broadening is density dependent the suppression of the cross section is reduced.

The effects noted above carry over to the case where only the final state interactions of the eta meson are taken into account. This latter case is relevant to the calculation of the inclusive cross sections on nuclei.

In conclusion we have shown the importance of including non-local effects in the relativistic calculations of the cross section for quasifree exclusive photoproduction of eta mesons on nuclei. In this framework this allowed us to probe the dependence of the cross section on interactions with the medium or alternatively on changes in the mass and width of the S_{11} resonance. This may open the way to using our present model to investigate these medium effects in relation to data on the inclusive reaction on nuclei (note that the cross sections for the exclusive reaction are rather small). Currently data that extend over a useful photon energy range exist only for the ^{12}C nucleus. We are in the process of analyzing these data. However it is desirable that the range of energies for existing data on other nuclei be extended to allow their inclusion in such analyses.

ACKNOWLEDGEMENTS

Two of the authers (M.H. and S.B.) whish to acknowledge the support of Faculty of Science Tehran University.

REFERENCES

[1] M. Benmerrouche, Nimai C. Mukhopadhyay, and J.F. Zhang, Phys. Rev. D**51**, (1995) 3237

[2] L. Tiator, D. Drechsel, G. Knöchlein and C. Bennhold, Phys. Rev. C**60** (1990)035210.

[3] A. Fix and H. Arenhövel, Nucl. Phys. **A620**, (1997) 457

[4] B. Krusche *et al.*, Phys. Lett. **358** (1995)40.

[5] M. Roebig-Landau *et al.*, Phys. Lett. **B373** (1996) 45.

[6] T. Yorita *et al.*, Phys. Lett. **476** (2000) 226.

[7] A. Fix and H. Arenhövel, Phys. Lett. **B492** (2000)32.

[8] W. Peters, H. Lenske and U. Mosel, Nucl. Phys. **A640**, (1998) 89.

[9] M. Hedayati-Poor and H.S. Sherif, Phys. Rev. C**56**, (1997) 1557.

[10] M. Hedayati-Poor and H.S. Sherif, Phys. Rev. C **58** (1998) 326.

[11] I.R. Blockland and H.S. Sherif, Nucl. Phys. **A694** (2001) 337.

[12] W. Peters, H. Lenske and U. Mosel, Nucl. Phys. **A642**, (1998) 506.

[13] J. Piekarewicz, A.J. Sarty and M. Benmerrouche, Phys. Rev. c**55** (1997) 2571; L.J. Abu-Raddad, J. Piekarewicz, A.J. Sarty and M. Benmerrouche, Phys. Rev. C**57** (1998) 2053.

[14] F.X. Lee, L.E. Wright, C. Bennhold and L. Tiator, Nucl. Phys. **A603** (1996) 345.

[15] E.D. Cooper and O.V. Maxwell , Nucl. Phys. **A493**, (1989) 486.

[16] J.I. Johansson and H.S. Sherif, Nucl. Phys. **A575**, (1994) 477.

[17] B.D. Serot and J.D. Walecka, *Advances in Nuclear Physics*, edited by J.W. Negele and E. Vogt, **16** (1986) 1.

[18] C.J. Horowitz and B.D. Serot, Nuc. Phys. **A368** (1986) 503.

[19] E.D. Cooper, S.Hama, B.C. Clark, and R.L. Mercer, Phys. Rev. C**47**, (1993) 297.

[20] H.C. Chiang, E. Oset and L.C. Liu, Phys. Rev. C**44** (1991)738.

[21] M. Effenberger and U. Mosel, nucl-th/9707010

[22] B. Krusche *et al.*, Phys Rev. Lett. **74** (1995) 3736.

[23] J. Lehr and U. Mosel, Phys. Rev. C**64** (2001)042202.

[24] K. Saito and A. W. Thomas, Phys. Rev. C**51** (1995)2757.

FIGURE CAPTIONS

FIG. 1. The cross section for the $^{12}C(\gamma,\eta p)^{11}B_{g.s.}$ reaction at photon energy of 750 MeV, plotted as a function of the kinetic energy of the outgoing η meson. Solid curve : non-local DW calculations (curve labeled DW(NL)). Dashed curve : local DW calculations (curve labeled DW(L)). Dotted curve : local PW calculations (curve labeled PW(L)). In this and all the subsequent figures S_{11} dominance is assumed.

FIG. 2. The cross section for the $^{40}Ca(\gamma,\eta p)^{39}K_{g.s.}$ reaction at 750 MeV. Only DW calculations are presented; solid curve : non-local DW calculations; dashed curve : local DW calculations.

FIG. 3. Same reaction as Fig.1. Distorted waves are used for the etas but protons are described by plane waves. Solid curve : non-local calculations; dashed curve : local calculations.

FIG. 4. Same reaction as Fig.1. Solid curve : calculations using a free propagator for S_{11} (curve labeled No ME). Dashed curve : the resonance interacts with medium via Hartree scalar potential (curve labeled S(r) Hartree). Dotted curve : the resonance interacts with medium via Hartree scalar and vector potentials (curve labeled S(r)+V(r) Hartree).

FIG. 5. Same reaction as Fig.1. Solid curve : calculations using a free propagator with width $\Gamma = 150$ MeV for S_{11}; dotted curve : $\Gamma = 208$ MeV. Dashed curve : calculations with a density dependent width (see text).

FIG. 6. Same reaction as Fig.1. Dotted curve : calculations using a free propagator for S_{11} (curve labeled No ME). Dashed curve : calculations with density dependent mass for S_{11} (curve labeled M(ρ_B)). Solid curve : calculations including density dependence for both mass and width of S_{11}.

FIG. 7. Same reaction as Fig.3. Dotted curve : calculations using a free propagator for S_{11}. Long-dashed curve : calculations with density dependent mass for S_{11}. Short-dashed curve :

calculations with density dependent width for S_{11}. Solid curve : calculations include density dependence for both mass and width of S_{11}.

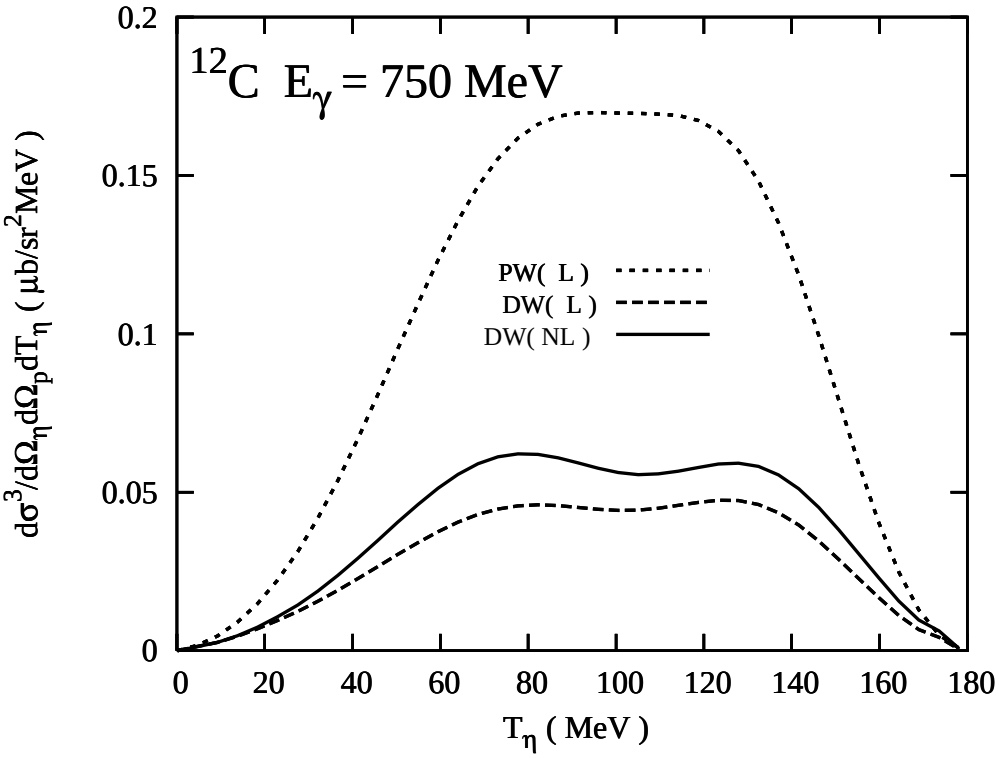

Fig. 1

M. Hedayati-Poor

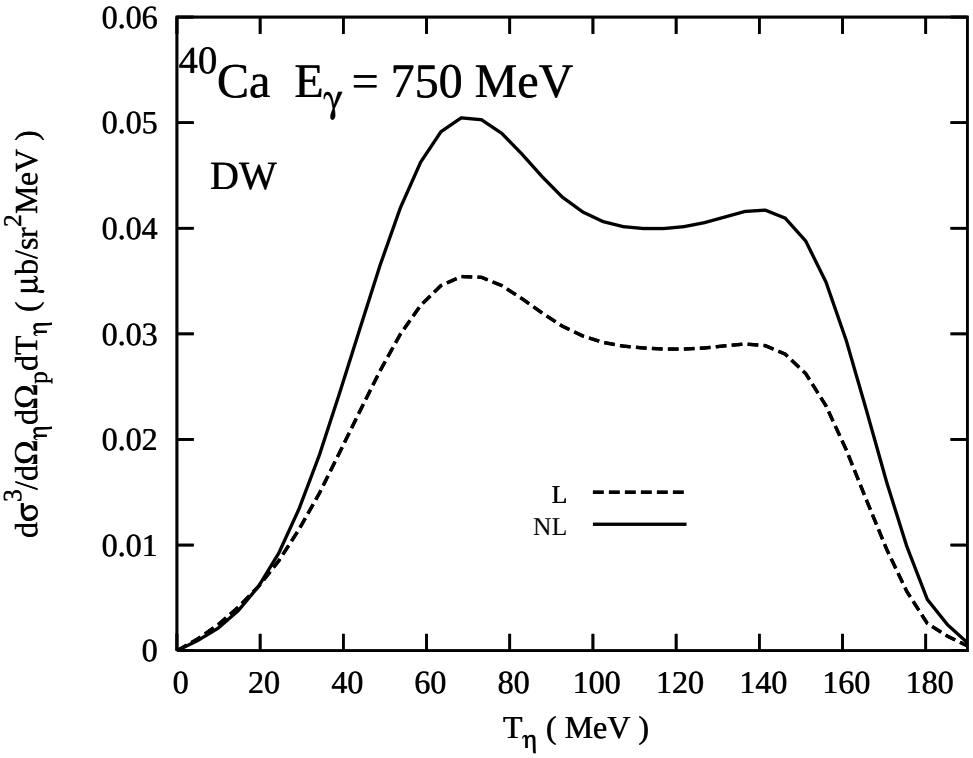

Fig. 2

M. Hedayati-Poor

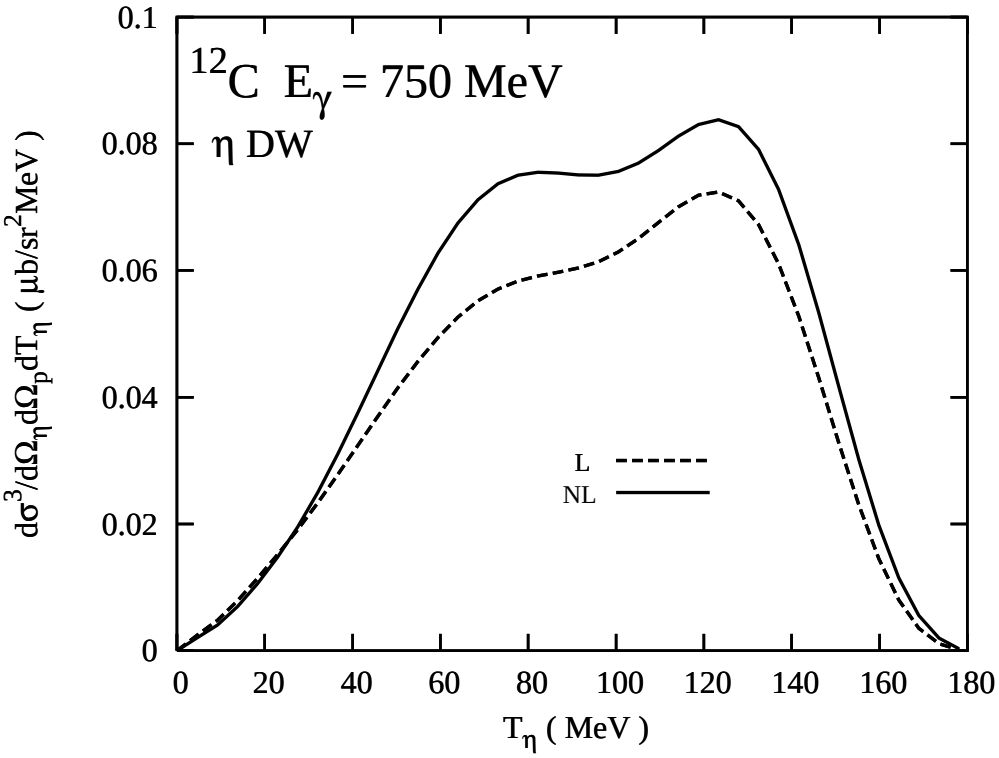

Fig. 3

M. Hedayati-Poor

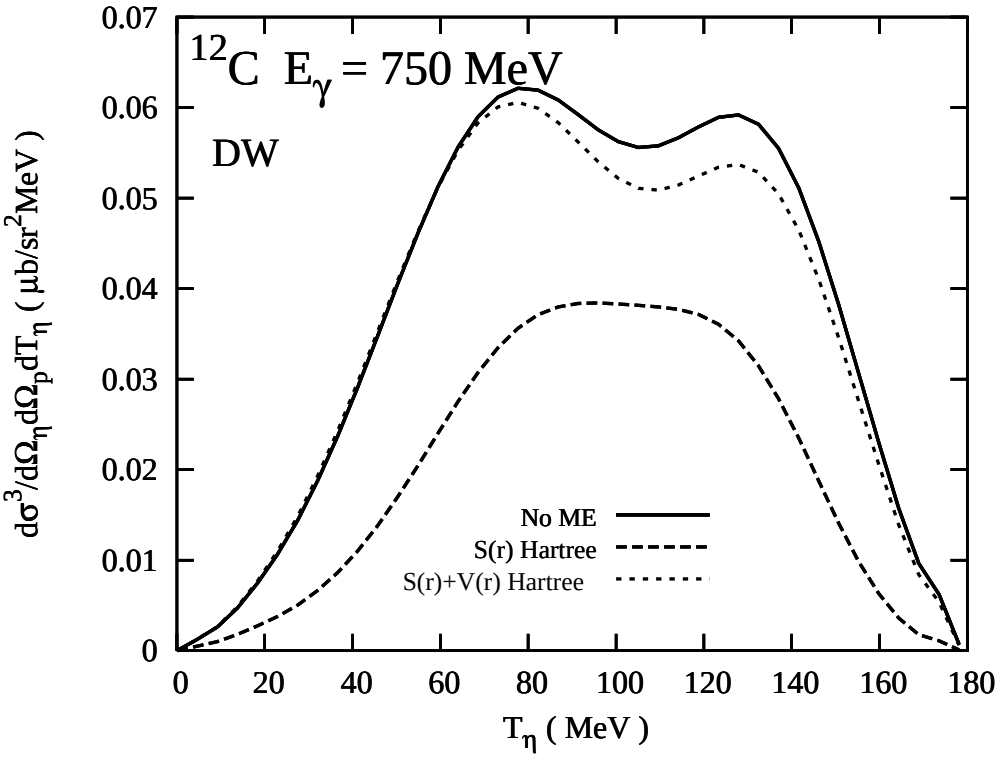

Fig. 4

M. Hedayati-Poor

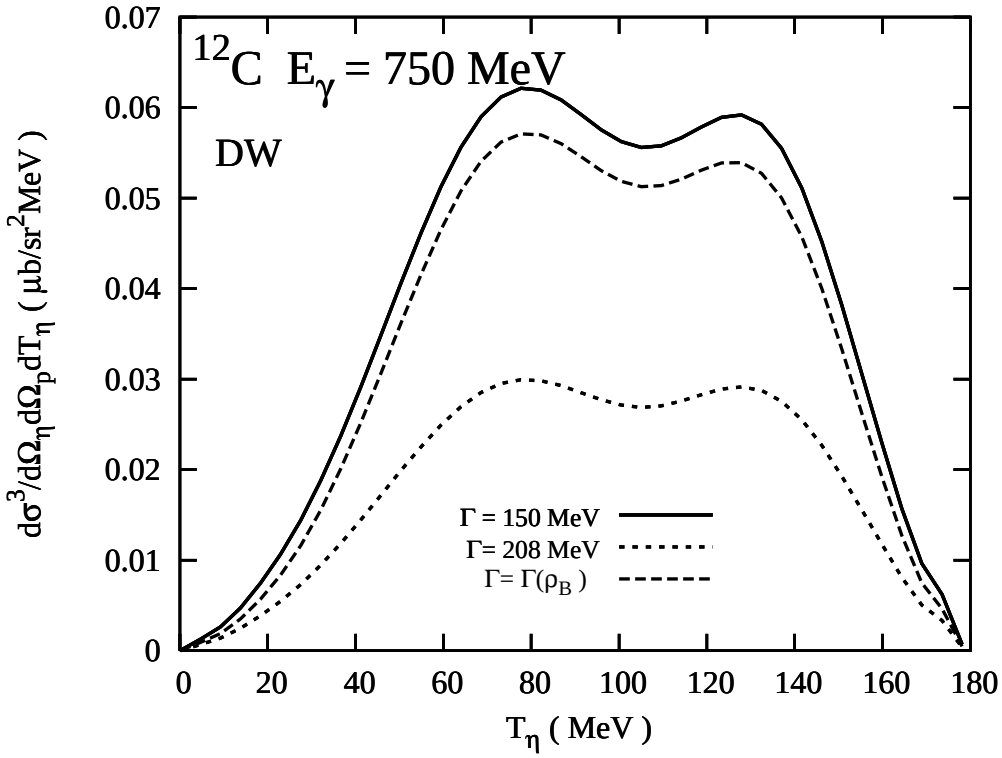

Fig. 5

M. Hedayati-Poor

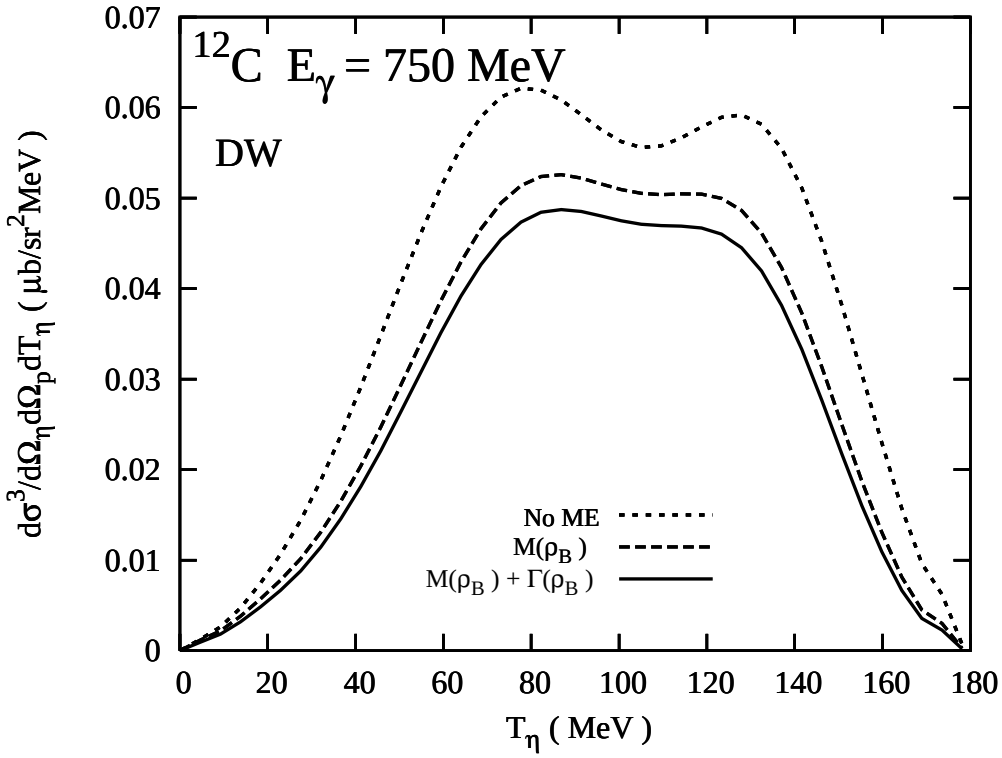

Fig. 6

M. Hedayati-Poor

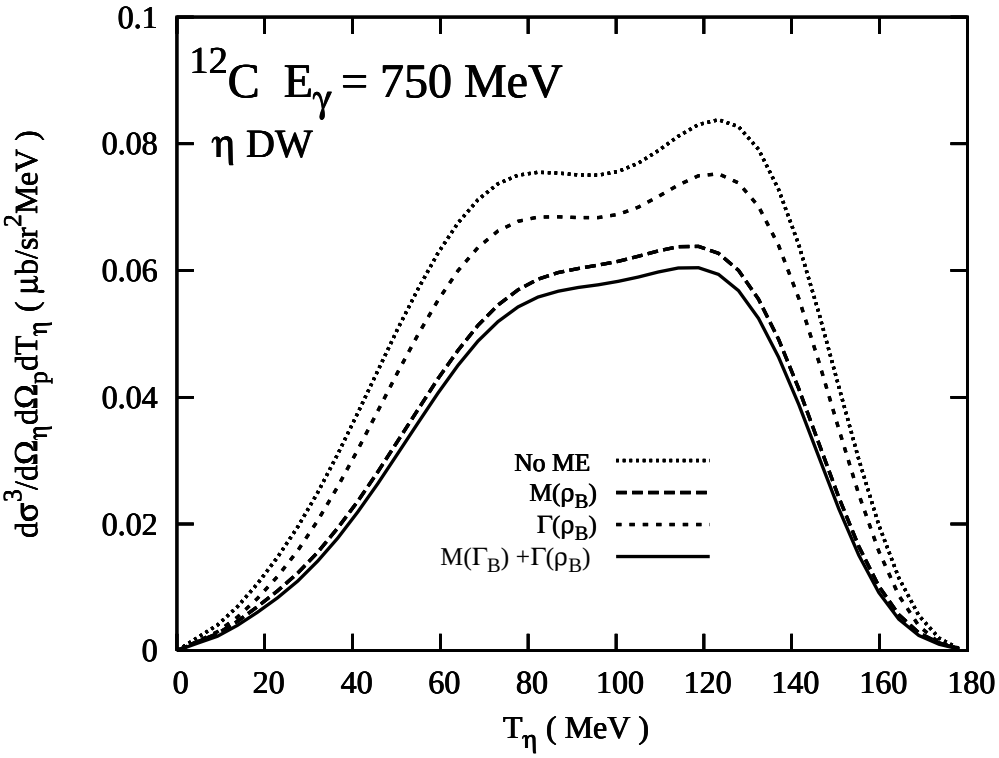

Fig. 7

M. Hedayati-Poor